

RESEARCH ARTICLE

Open Access



Comparative morphology and development of extra-ocular muscles in the lamprey and gnathostomes reveal the ancestral state and developmental patterns of the vertebrate head

Daichi G. Suzuki^{1*}, Yuma Fukumoto^{2,3,4}, Miho Yoshimura¹, Yuji Yamazaki⁵, Jun Kosaka^{3,6}, Shigeru Kuratani² and Hiroshi Wada¹

Abstract

The ancestral configuration of the vertebrate head has long been an intriguing topic in comparative morphology and evolutionary biology. One peculiar component of the vertebrate head is the presence of extra-ocular muscles (EOMs), the developmental mechanism and evolution of which remain to be determined. The head mesoderm of elasmobranchs undergoes local epithelialization into three head cavities, precursors of the EOMs. In contrast, in avians, these muscles appear to develop mainly from the mesenchymal head mesoderm. Importantly, in the basal vertebrate lamprey, the head mesoderm does not show overt head cavities or signs of segmental boundaries, and the development of the EOMs is not well described. Furthermore, the disposition of the lamprey EOMs differs from those the rest of vertebrates, in which the morphological pattern of EOMs is strongly conserved. To better understand the evolution and developmental origins of the vertebrate EOMs, we explored the development of the head mesoderm and EOMs of the lamprey in detail. We found that the disposition of lamprey EOM primordia differed from that in gnathostomes, even during the earliest period of development. We also found that three components of the paraxial head mesoderm could be distinguished genetically (premandibular mesoderm: *Gsc*+/*TbxA*-; mandibular mesoderm: *Gsc*-/*TbxA*-; hyoid mesoderm: *Gsc*-/*TbxA*+), indicating that the genetic mechanisms of EOMs are conserved in all vertebrates. We conclude that the tripartite developmental origin of the EOMs is likely to have been possessed by the latest common ancestor of the vertebrates. This ancestor's EOM developmental pattern was also suggested to have resembled more that of the lamprey, and the gnathostome EOMs' disposition is likely to have been established by a secondary modification that took place in the common ancestor of crown gnathostomes.

Keywords: Evo-devo, Extra-ocular muscles, Lamprey, Head mesoderm, Head segmentation

* Correspondence: daichi1207@gmail.com

¹Graduate School of Life and Environmental Sciences, University of Tsukuba, 1-1-1 Tennodai, Tsukuba, Ibaraki 305-8572, Japan

Full list of author information is available at the end of the article



Introduction

The morphological nature and ancestral configuration of the vertebrate head are longstanding topics of interest in comparative morphology and evolutionary biology. A peculiar component of the vertebrate head is the extra-ocular muscles (EOMs), which control the visual field by the moving eyes. These muscles are derived from the paraxial portion of the head mesoderm, and their development has attracted the attention of morphologists in the context of head mesodermal segmentation.

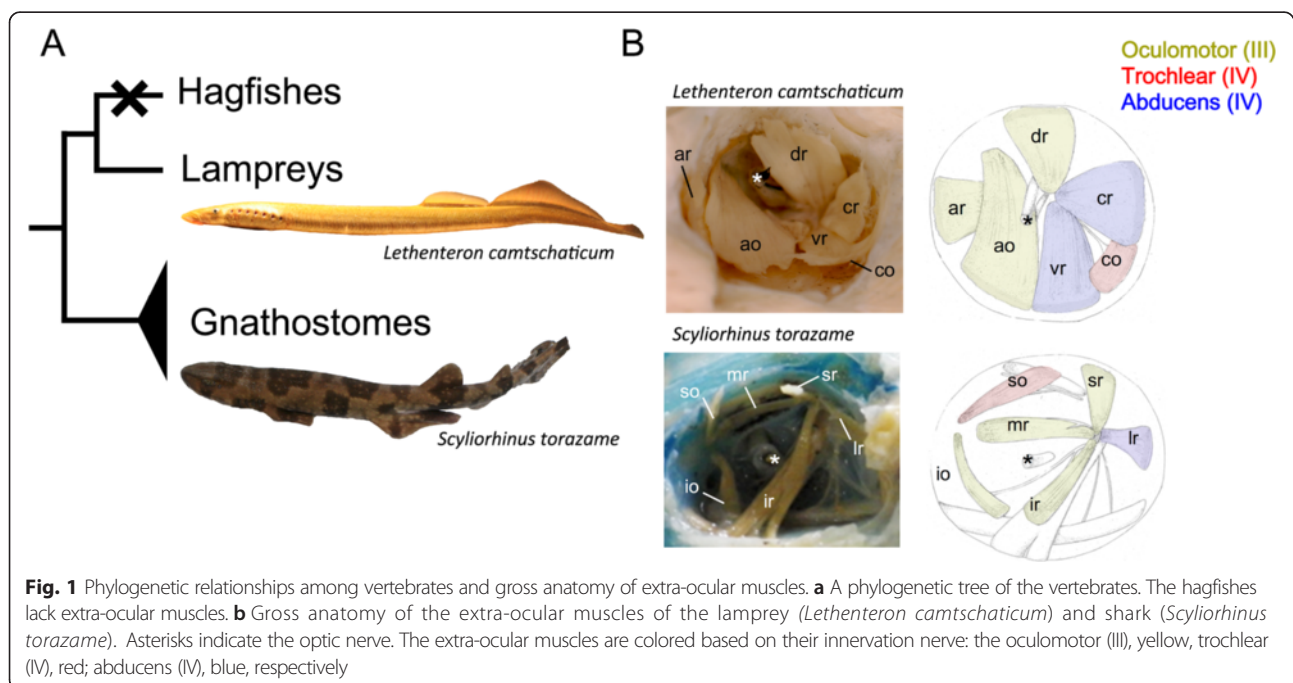
Some researchers believe that these muscles are derived from rostral mesodermal segments of an amphioxus-like ancestor (reviewed in [1–4]). This idea partially stems from the presence of the epithelialized head mesodermal cysts (head cavities) in the shark embryo [5]; the head mesoderm in elasmobranch embryos typically forms three pairs of head cavities, from anterior to posterior, the premandibular (pc), mandibular (mc), and hyoid cavities (hc). These cavities later differentiate into six EOMs innervated by three cranial nerves: the oculomotor (III), trochlear (IV), and abducens nerves (VI) (Fig. 1). Although a complete set of head cavities arises only in cartilaginous fishes, they are occasionally found in osteichthyans including amniotes [6–15]. This indicates that possession of these cavities is a shared, derived characteristic for gnathostomes, although they tend to disappear in many osteichthyan taxa.

In avians, the head cavities have disappeared except for the remnant premandibular cavity [16–18]. In a different line of studies, a series of pseudosegmental blocks,

so-called “somitomeres”, have been detected by scanning electron microscopy in the early head mesoderm, in which no head cavities are expected to arise (reviewed in [17]). Although the existence of the somitomeres has been questioned (reviewed in [3]), the EOMs do develop from a part of the head mesoderm corresponding to the sites of head cavities in elasmobranchs [11, 18–24].

Classically, the head mesoderm of lampreys, which belong to the most basal group of vertebrates (cyclostomes), was also thought to be segmented along the anteroposterior axis, similar to that in the head cavities in elasmobranch embryos [25–27], and EOMs were thought to differentiate from the three head cavities, innervated by their respective motor nerves [25, 26]. However, scanning electron microscopy-based observations of the Arctic lamprey, *Lethenteron camtschaticum* by Kuratani et al. [28], show no signs of segmental boundaries in the dorsal (paraxial) head mesoderm. Rather, the dorsal head mesoderm was simply secondarily regionalized into preotic and postotic portions by the otic vesicle, and the ventral part segmented passively by the pharyngeal pouches, in accordance with the notion of branchiomery proposed by Sewertzoff [29]). This finding suggests that the ancestral head mesoderm of the vertebrates is likely to have been unsegmented in the paraxial portion, raising the question of how the EOMs developed from this unsegmented head mesoderm.

The anatomical disposition and the innervation patterns of EOMs are highly conserved among gnathostomes, so much so that Neal [26] once noted that “[t]heir ‘evolutionary potential’ appears to be approximately zero”. However,



the patterns of lamprey EOMs have been known to differ from living gnathostomes (Fig. 1, [30–32]). In the latter, the oculomotor nerve innervates four of the EOMs (medial rectus (mr), superior rectus (sr), inferior rectus (ir), and inferior oblique (io)), whereas the trochlear and abducens innervate only single EOMs (superior oblique (so) and lateral rectus (lr), respectively). In contrast, the lamprey oculomotor nerve innervates only three EOMs (anterior rectus (ar), dorsal rectus (dr), and anterior oblique (ao)), while the abducens innervates two (ventral rectus (vr) and caudal rectus (cr)). Furthermore, the caudal oblique (co) muscles of lampreys, which are innervated by the trochlear nerve, attach to the orbit far more caudally than do those of modern gnathostomes. Because the EOMs have degenerated completely in hagfishes [32], the lamprey is the only key extant animal to speculate ancestral state of the EOMs and its developmental mechanisms.

To understand the evolutionary origin of the vertebrate EOMs and suggest a possible ancestral state of the vertebrate head, we examined the development of the embryonic head mesoderm and EOMs in lampreys. We found that the developmental pattern of EOMs was also conserved in the lamprey, because the muscle originated from three domains along the anteroposterior axis in the dorsal (paraxial) head mesoderm. However, EOM disposition was different between lampreys and gnathostomes, as soon as EOMs were observed as differentiated muscles. These findings indicate that the developmental mechanisms of EOMs from the three subdivisions of the head mesoderm was already established in the common ancestor of vertebrates, and that diversification of the muscle patterns is due to changes during the later phase of development. Based on these findings, we discuss the ancestral state of the vertebrate dorsal head mesoderm and its differentiation.

Materials and methods

Animals

This study was performed in accordance with the Regulations on Animal Experimentation at University of Tsukuba. Approval is not needed for experimentation on fishes under Japanese law, Act on Welfare and Management of Animals.

Adult lampreys (*Lethenteron camtschaticum*, synonym *L. japonicum*) were collected from the Shiribeshi-Toshibetsu River, Hokkaido, Japan. The animals were anesthetized in ethyl,3-aminobenzoate methanesulfonate (MS-222). Mature eggs were squeezed from females and fertilized in vitro by sperm. Embryos were cultured at 16 °C, fixed in 4 % paraformaldehyde in 0.1 M phosphate-buffered saline (PBS) overnight, dehydrated in a graded methanol series, and stored in 100 % methanol at –20 °C. Developmental stages were determined as described by Tahara [33].

As ammocoete larvae were not readily available for *L. camtschaticum*, we used larvae from *Lethenteron* sp. N,

related species of *L. camtschaticum* [34, 35]. These larvae were collected from the Kamo River, which flows through the middle of the Shougawa River, Toyama, Japan, in September.

Fertilized eggs of the cloudy catshark (*Scyliorhinus torazame*) were obtained from adults that were bred at 16 °C in seawater tanks. Shark embryos were staged following Ballard's staging of *Scyliorhinus canicula*, a species closely related to *S. torazame* [36, 37].

Histological analyses

Lethenteron sp. N and *Scyliorhinus torazame* were fixed in Bouin's or Serra's fixative, dehydrated, and embedded in paraffin. Sections were cut at a thickness of 6 µm and stained with hematoxylin and eosin, following a standard protocol.

3D reconstruction

The stained sections of *Lethenteron* sp. N and *S. torazame* were digitized using an Olympus BX60 microscope equipped with an Olympus DP70 camera and the Olympus DP controller software (Olympus, Tokyo, Japan). On the digitized sections, each anatomical component was colored and reconstructed using the Avizo 3D Visualization Framework (Maxnet Co., Ltd, Tokyo, Japan).

Whole-mount immunofluorescence

Whole-mount immunofluorescence with anti-acetylated tubulin (Sigma, T6793) and anti-tropomyosin (Hybridoma bank, CH1) antibodies was performed according to the protocol described by Kuratani et al. [38] with some minor modifications. Briefly, fixed embryos stored in methanol were washed in TBST containing 5 % dimethylsulfoxide (TSTd). The embryos were then blocked with 5 % non-fat dry milk in TSTd (TSTM). They were incubated with the primary antibody (diluted 1:1,000 in TSTM) for 2–4 days at room temperature (RT). After washing with TSTd, samples were incubated with a secondary antibody (Invitrogen, Alexa fluor 555, A21424) diluted 1:200 in TSTM. After a final wash in TSTd, embryos were dehydrated and clarified in a 1:2 mixture of benzyl alcohol and benzyl benzoate (BABB) and then examined using a confocal laser microscope (LSM 510, Zeiss). The data were colored and projected by using a computational graphics editor (Photoshop CS6).

Whole-mount and section in situ hybridization

Gsc was amplified from *L. camtschaticum* by RT-PCR from stage 25 specimens using the primers designed for *Petromyzon* genes (*PmGsc*, HQ248103) [39]. For the other genes, probes were synthesized by using the plasmids in accordance with previously described protocols (*PitxA*: Uchida et al. [40]; *MrfA*, *MA2*: Kusakabe et al. [41]; *Tbx1/10*: Tiecke et al. [42]). Whole-mount in situ

hybridization was performed according to the protocol of Ogasawara et al. [43] with minor modifications. For section in situ hybridization, larval lampreys (*L. sp. N*) were fixed for three days in 4 % paraformaldehyde in 0.1 M phosphate-buffered saline (PBS), dehydrated, and embedded in paraffin. Sections were cut at a thickness of 8 μm . After washing out the paraffin, in situ hybridization for cryosectioned materials was performed following the protocol for whole-mount in situ hybridization, except that Tween 20 was not used at any step and proteinase treatment was omitted before hybridization.

Cell labeling

St. 21 embryos were injected with 1 mM DiI, DiD, and DiO solutions (Vybrant Multicolor Cell-labeling kit, Molecular Probes). The embryos were excised from the egg membranes and placed in wells made in solidified agar on a plastic dish. Injections were performed with a fine glass pipette. The embryos were incubated for 10 days until st. 27 was approximately reached and were fixed in 4 % paraformaldehyde in PBS. Observation was made with a fluorescence microscope or confocal microscope (LSM510, Zeiss, Goettingen, Germany).

Results

Development of the EOMs and their innervation

To clarify the disposition and innervation pattern of EOMs in lamprey larvae, we first performed 3D reconstruction of a ca. 100 mm ammocoete larva (Fig. 2a–d). At this stage, six EOMs were already differentiated as distinct muscle primordia attached to the surface of the eye (Fig. 2a). They consisted of four rectus muscles (ar, dr, cr, and vr) and two oblique muscles (ao and co). This muscle organization was the same as that known in the adult lamprey (Fig. 1b, [30–32]). To confirm the muscle identities, we also analyzed the innervation patterns of these EOMs. As reported for adult specimens (Fig. 1b, [30–32]), the oculomotor nerve (III) innervated the ‘ar’, ‘dr’, and ‘ao’ muscles (Fig. 2b), the trochlear nerve (IV) the ‘co’ muscle (Fig. 2c), and the abducens nerve (VI) the ‘vr’ and ‘cr’ muscles (Fig. 2d). Notably, the pathways of the trochlear and abducens nerves partially overlapped those of the trigeminal nerve (V), and the trochlear nerve ramifies into sub-bundles and become fasciculated again near its terminus (Fig. 2c). We confirmed this observation by immunofluorescence analysis using an anti-acetylated tubulin antibody in early larvae, as described below. Furthermore, the attachment site of the ‘ao’ muscle to the cartilaginous orbital wall was

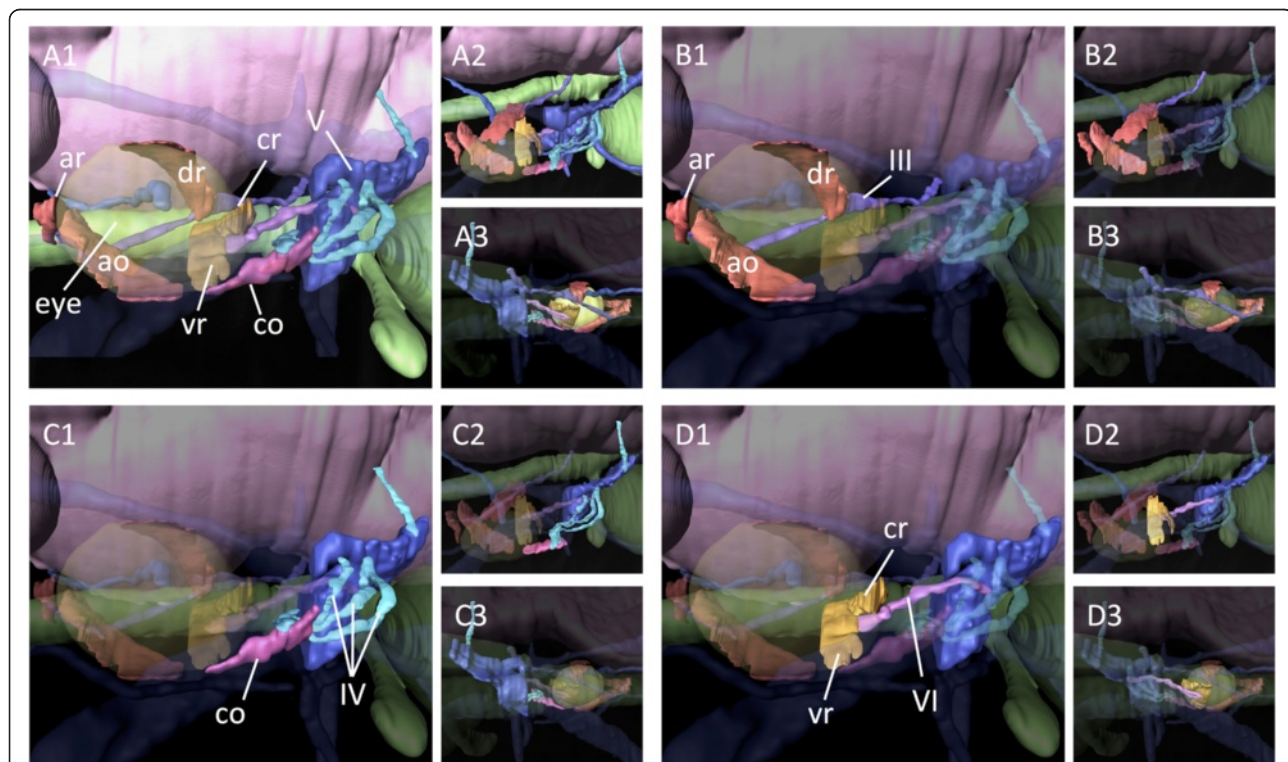


Fig. 2 3D reconstruction of a lamprey ammocoetes larva. **a** Overview. **b** The oculomotor nerve and its innervating extra-ocular muscles. **c** The trochlear nerve and its innervating caudal oblique muscle. **d** The abducens nerve and its innervating extra-ocular muscles. **a1–d1**: Lateral; **a2–d2**: Dorsal; **a3–d3**: Medial view

relatively more ventral (Fig. 2b) than that in the adult, in which the ‘ao’ muscle crossed over the ‘ar’ muscle (Fig. 1).

For the comparison, we constructed 3D images of a pre-hatching stage (72 mm long) embryonic shark (*Scyliorhinus torazame*) to represent gnathostomes (Fig. 3a–d). Consistent with the adult anatomy (Fig. 1b) as well as previous descriptions [30–32], the oculomotor nerve (III) innervated the ‘mr’, ‘sr’, ‘ir’, and ‘io’ muscles (Fig. 3b), the trochlear nerve (IV) the ‘so’ muscles (Fig. 3c), and the abducens nerve (VI) the ‘lr’ muscles (Fig. 3d). The ciliary ganglion was observed in the orbit (inset in Fig. 3b1), but no similar ganglion was found in the lamprey (Fig. 2).

To determine whether the disposition of the lamprey EOMs changes during development, we performed a histological analysis by hematoxylin and eosin (HE) staining in stage (st.) 30 prolarvae (Fig. 4), 35 mm (about half a year old, Fig. 5a), 100 mm larvae (Fig. 5b), metamorphic (Fig. 5c) and adult lampreys (Fig. 5d). In st.30 prolarvae, we found no muscle fibers suggestive of EOM differentiation, but only mesenchymal cell masses surrounding the eyeball (Fig. 4).

In the 35 mm larvae, EOMs were found as fibrous, distinguishable six-cell clusters (Fig. 5a), identities of which

were obvious from their disposition. Rectus muscles were located at the anterior, dorsal, ventral, and caudal parts in the orbit; thus, we named them the anterior, dorsal, ventral, and caudal rectus muscles, respectively. As for two oblique muscles, one primordium originated slightly ventral to ‘ar’, and was directed caudally; it was therefore identified as the ‘ao’ muscle. The other, identified as the ‘co’, originated from the dorsocaudal region in the orbit, was directed ventrally.

In the 100 mm larvae, the EOMs become more clearly compartmentalized and discriminable (Fig. 5b), suggesting the growth of the EOMs of this animal during the larval period, ranging 4–5 years. The topological disposition of the EOMs was the same as that in the 35 mm larvae. In the metamorphic stage, the external part of the EOMs became thinner and wider (Fig. 5c1), suggesting rigid attachment to the eyeball to exert its functional movement. The relatively immature state of larval EOMs may be due to the larval life style of this animal, in which the eyes do not possess image-forming vision [44–47]. Through all of the stages examined, the positions of the EOMs did not show radical changes, and it seemed likely that the EOM morphological pattern is established during the pre-metamorphic stages. However, the little change in the relationship between the ‘ar’

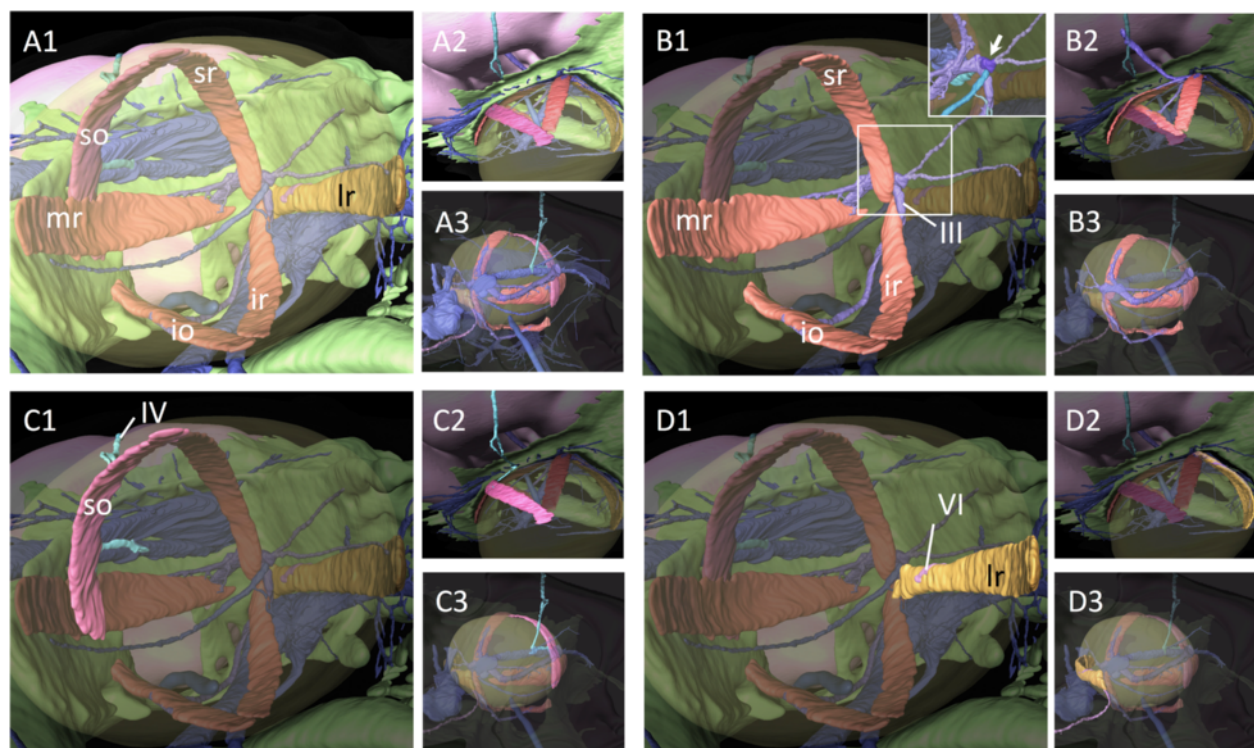


Fig. 3 3D reconstruction on *Scyliorhinus torazame*. **a** Overview. **b** The oculomotor nerve and its innervating extra-ocular muscles. **a** detailed structure of oculomotor nerve (III) is shown in the inset, in which a ciliary ganglion-like structure is indicated by an arrow and highlighted in blue color. **c** The trochlear nerve and its innervating superior oblique muscle. **d** The abducens nerve and its innervating lateral rectus muscle. **a1–d1**: Lateral; **a3–d3**: Dorsal; **a3–d3**: Medial view

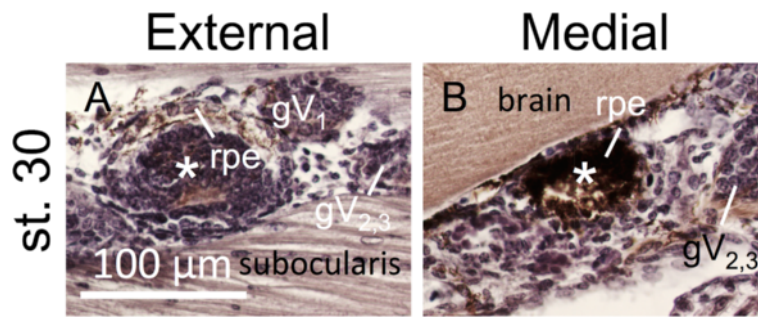


Fig. 4 Histological analysis by the hematoxylin and eosin (HE) staining on the extraocular muscles in st. 30 prolarva. Asterisks indicates the eye. **a** External section. **b** Medial section

and ‘ao’ muscles was notable. During the larval period, these muscles at first run in parallel to each other (Fig 2a4, Bb), and cross each other in the adults (Figs. 1b and 5d4). This change is likely to occur during metamorphosis.

Developmental mechanism of EOMs and patterning of head mesoderm

To trace further the developmental origin of the lamprey EOMs, immunofluorescence analysis was performed using an anti-tropomyosin antibody in younger lamprey larvae (Fig. 6a–c). We did not detect any EOMs in st. 28 or st. 30 prolarvae, but did detect other muscles,

including somatic/branchial muscles; supraocularis, subocularis, elevator labialis ventralis (elv), velocranialis, and constrictor buccalis (Fig. 6a, b, see also [48]).

Next, we traced the developmental origin of EOMs by analyzing more upstream regulatory genes for EOMs. In gnathostomes, the genetic cascade involved in the development of EOMs has already been reported; genes encoding muscle-related factors (MRFs) act as determination and differentiation genes, *Pitx2* acts upstream of MRFs in cranial muscle progenitor cells, and *Pitx2*-null embryos lack EOMs [49]. This cascade is also conserved in sharks, in which *Pitx2* and *Myf5* (a member of the MRF family) are expressed in developing head mesoderm/cavities [50].

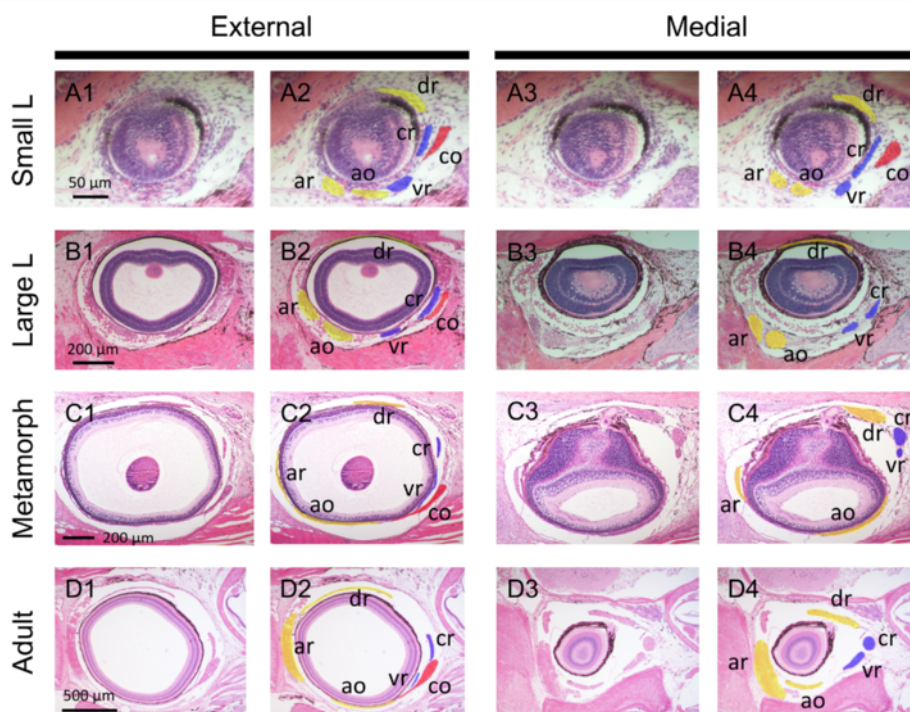


Fig. 5 Histological analysis by hematoxylin-eosin (HE) staining of the extraocular muscles in larval, metamorphic and adult lampreys. **a** Small larva (3.5 cm, about half a year old). **b** Large larva (10 cm). **c** Metamorphic lamprey. **d** Adult lamprey **a1–d1**: External sections; **a2–d2**: External sections, colored; **a3–d3**: Medial sections; **a4–d4**: Medial sections, colored

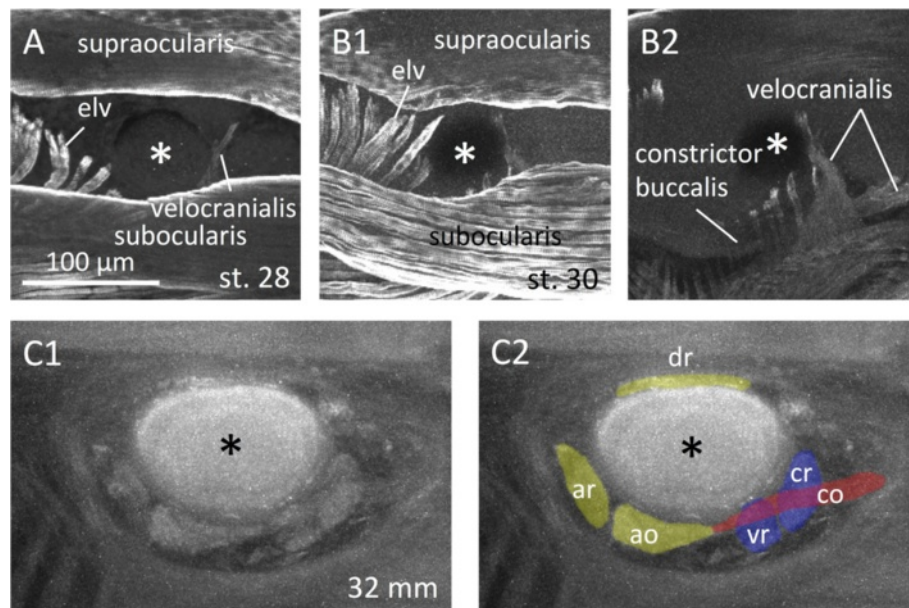


Fig. 6 Whole-mount immunofluorescence with an anti-tropomyosin antibody. Asterisks indicates the eyes. **a** st. 28 prolarvae. **b** st. 30 prolarvae (**b1**: Overview; **b2**: Medial). **c** 32 mm larva (**c1**: Raw; **c2**: Colored)

In a st. 26 prolarva, although *MrfA* (a member of the MRF family) and *MA2* (a muscle differentiation marker) were not expressed [41], we detected *Pitx2* transcripts in the head mesoderm (Fig. 7a). In contrast, in the 90 mm ammocoete larvae, *MrfA* and *MA2* were expressed in EOM primordia, while the *Pitx2* expression ceased (Fig. 8).

Furthermore, we found that there was distinct genetic regionalization in the dorsal head mesoderm. In gnathostomes, *Gsc* is expressed in the prechordal plate [51], from which the premandibular mesoderm (pm) is thought to arise (lampreys: [28]; sharks: [36]). *Gsc* plays a dominant role as an organizer in head formation, including head muscle differentiation [52]. We found that *Gsc* was expressed in the anteriormost head mesoderm in the st. 26 lamprey prolarvae (Fig. 7b), and expression corresponded to that in the premandibular mesoderm. Simultaneously, *TbxA* transcripts were detected in the paraxial head mesoderm located anterior to the otic vesicle (Fig. 7c). In sharks, an equivalent expression has been observed in the hyoid cavity [50]. In the mouse, *Tbx1* (homolog of the lamprey *TbxA*) regulates craniofacial myogenesis [53]. Thus, *TbxA* expression in the lamprey is expected to represent that in the paraxial portion of the hyoid mesoderm (hm). These results suggest that the dorsal head mesoderm of lamprey, characterized by *PitxA* expression along the anteroposterior axis, is further specified through expression of *Gsc* and *TbxA*, i.e., pm: *Gsc*⁺, *TbxA*⁻; mm: *Gsc*⁻, *TbxA*⁻; hm: *Gsc*⁻, *TbxA*⁺ (Fig. 7d).

Developmental lineage of the head mesoderm: origin of the differentiated EOMs

On examination of expression of *Pitx*, *Gsc*, and *Tbx*, three distinct domains were identifiable in the lamprey dorsal head mesoderm, in a pattern similar to those in gnathostomes. Thus, via immunofluorescence analysis using an anti-acetylated tubulin antibody, we examined differentiation of the three lamprey head mesodermal portions into the specific EOM groups innervated by the respective cranial motor nerves as seen in shark head cavities [5]. In the st. 28 prolarva, although the head mesoderm was not differentiated into the EOMs (Fig. 6a), *PitxA* was expressed in the three components of the dorsal head mesoderm (Fig. 9a). At this stage, the EOM-innervating nerves were already extending their fibers, and the distribution pattern corresponded to each portion of the dorsal head mesoderm: the oculomotor nerve (III) reached the premandibular mesoderm, the trochlear nerve (IV) the mandibular mesoderm, and the abducens nerve (VI) the hyoid mesoderm (Fig. 9b, c). These fibers approached the orbit in the 15 mm larvae (Fig. 9d), and their distribution pattern was maintained through the larval period, by which time the EOMs had already been formed (35 mm; Fig. 9e, see also Fig. 6c). These results indicate that the three components of the dorsal head mesoderm are assigned morphologically to respective nerves in a modern gnathostome pattern, and that nerve innervation is maintained through

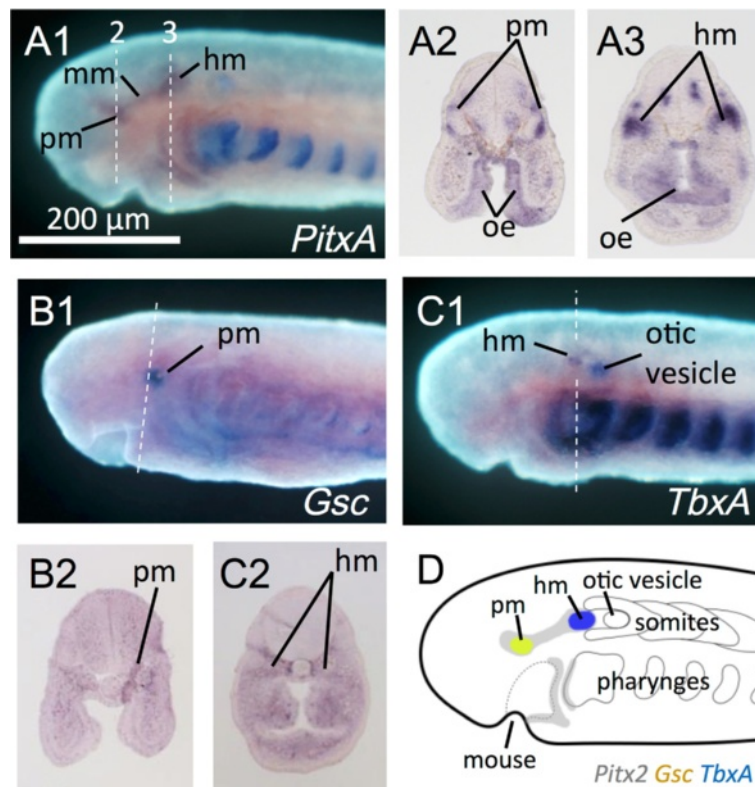


Fig. 7 Whole-mount in situ hybridization in st. 26 lamprey prolarvae. **a** *PitxA* (**a1**: Lateral view; **a2**, **3**: Sections). **b** *Gsc* (**b1**: Lateral view; **b2**: Section). **c** *TbxA* (**c1**: Lateral view; **c2**: Section). **d** Schematic illustration of the *PitxA*, *Gsc*, and *TbxA* expression patterns

differentiation into EOMs, supporting differentiation of the specific paraxial head mesodermal portion into specific subsets of EOMs.

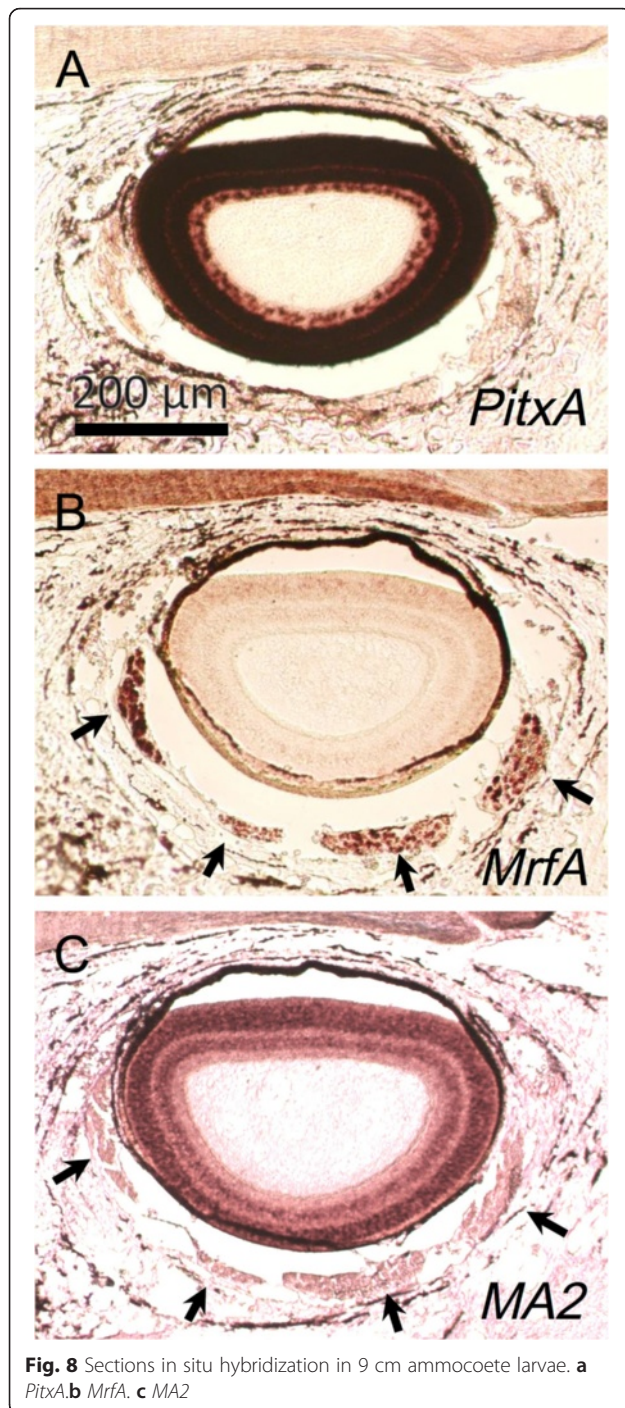
In lamprey development, the premandibular mesoderm is derived from the prechordal plate, and the mandibular and hyoid mesoderm are regionalized rostrocaudally from each other by the growth of the first pharyngeal pouch [28]. Based on our results (Fig. 7), each of these subdivisions appears to correspond to a genetically-specified subdivision, as described above. However, there is another possibility that the mesenchymal cells are mixed and then become re-specified. Thus, we performed cell-labeling experiments to determine whether each head mesodermal portion retained its cohesion from its origin or became mixed. First, only DiO was injected into the prechordal plate region in st. 21 embryos (Fig. 10a) and incubated until st. 27. At st. 27, a DiO signal was observed around the eyeball, although the eyeball itself was also labeled as an artifact (Fig. 10b, c). Subsequently, triple dye injections were performed; DiO was injected into the prechordal plate, DiI into the mandibular mesoderm, and DiD into the hyoid mesoderm in st. 21 embryos (Fig. 10d). The mesodermal portions retained their cohesion and did not mix with each other in almost all of the

larvae at st. 27 ($n = 43/48$; no fluorescent signal was detected in the remaining 5 samples), (Fig. 10e). The positions of these mesodermal portions also corresponded to the expression patterns of *Gsc* and *TbxA* as described above (Fig. 7d, e). These results indicate that the above noted dorsal head mesoderm is regionally specified early in development as well, with respect to their developmental fates.

Discussion

Developmental mechanism of the EOMs and the head mesoderm

The aim of the present study was to determine the evolutionary history of vertebrate EOMs. First we compared the disposition and nerve innervation of the EOMs between larval lampreys and shark embryos. The results showed that the disposition and nerve innervation patterns were quite different between these two animals (Figs. 2 and 3). We then traced the developmental process of the EOMs in lampreys using histological analysis. The overall disposition of the lamprey EOMs is established as early at 32 mm larvae (approximately six-months-old, Fig. 6c) in the paraxial (dorsal) head mesoderm, which is regionally and genetically specified during early stages of development (Figs. 4, 5 and 6). These



results indicate that the lampreys and gnathostomes show different distributions of EOMs as soon as they are observed as differentiated muscles (lamprey: Fig. 6c; chick: reviewed in [22]).

In contrast, we found that the genetic cascade involved in development seems to be conserved in the lamprey, and that the dorsal head mesoderm is first marked by the expression of *PitxA* (at st. 26, Fig. 7). Furthermore, the expression patterns of *Gsc* and *TbxA* (Fig. 7) suggest

that regionalization as well as specification of the three mesodermal portions underlie the distinct genetic characterizations. *Gsc* expression in the premandibular region is also observed in the zebrafish [54] and mouse [55], and *Tbx* expression has been observed in the dorsal hyoid region of the shark [50], zebrafish [56], *Xenopus* [57], chick [22], and mouse [58]. Thus, these expression patterns appear to be conserved among vertebrates. In addition, these mesodermal portions retain their cohesion and attract their respective innervating nerves (Figs. 9 and 10), similar to those in the shark head cavities [5], even if there is no morphological segmentation in the lamprey dorsal head mesoderm [28].

Since we did not detect any muscle differentiation markers such as the *MA2* gene or the anti-tropomyosin antibody during the developmental stage at which *Pitx*, *Gsc* and *Tbx* expressions were detected, it was unclear whether the *Pitx*-positive head mesoderm truly differentiated into EOMs in the lampreys. We circumvented this problem by examining head mesodermal innervation by motor nerves. We present evidence indicating that, although the muscle markers were not detected at the time *Pitx* expression was detected, motor innervation was observed at this stage. The oculomotor nerve fibers reached the premandibular mesoderm, the trochlear nerve the mandibular mesoderm, and the abducens nerve the hyoid mesoderm (Fig. 9b, c). This innervation pattern supported the hypothesis that lamprey EOMs differentiate from the three components of the dorsal head mesoderm.

Figure 11 shows a comparison of EOM development in lamprey and shark. In both species, the early head mesoderm is primarily uniform with no overt segmental patterns at paraxial levels (Fig. 11a, d, [28, 36]). However, it is specified into three components, each innervated by a single cranial nerve (cranial nerves III, IV, and VI; Fig. 11b, e). In the shark, these components correspond to three pairs of epithelial coeloms called head cavities [36]. Finally, the EOMs are formed in their lineage-specific dispositions (Fig. 11c, f). This comparison indicates that the derivation of EOMs from the three components of dorsal head mesoderm would have already been established by the latest common ancestor of vertebrates (Fig. 12).

Ancestral state of EOMs in vertebrates and subsequent evolutionary modifications in gnathostomes

The comparison of EOM development between lampreys and gnathostomes described above indicated that the evolutionary modification of EOMs would have been introduced into a developmental stage following establishment of the three dorsal head mesodermal portions, but preceding the start of muscle differentiation (corresponding to between st. 28 and the 35 mm early larval stage of lampreys).

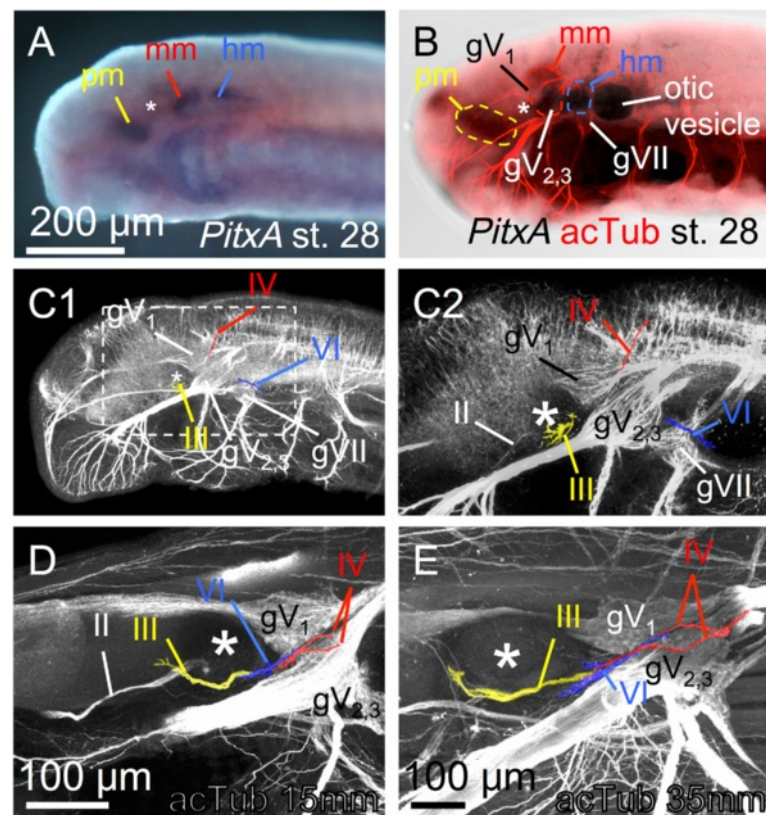


Fig. 9 Nerves innervating head mesodermal portions and EOMs. Asterisks indicate the eyes. **a** *PitxA* expression in st. 28. **b** Double-staining of *PitxA* in situ hybridization (bright field) and an anti-acetylated tubulin antibody immunofluorescence (red). **c**, **d** Single immunofluorescence with the anti-acetylated tubulin antibody. **c** st. 28 (**c1**: Overview; **c2**: magnified dashed box region in **c1**). **d** 15 mm larva. **e** 35 mm larva

However, the type of EOM distribution that represents the ancestral disposition of the vertebrates could not be determined in the present study, as there are only two groups with different EOM patterns (lampreys and extant gnathostomes), and both hagfishes and the outgroup (protochordates) lack EOMs. Nevertheless, previous studies on fossil records [59–62] analyzed the morphology of the orbit including distribution of myodomies (orbital wall depressions indicating muscle insertions) and suggested that the disposition of EOMs in osteostracans and placoderms would have been similar, to some extent, to that of lampreys than the extant gnathostomes. Based on recent phylogenetic analyses [63–65], the pattern of EOM disposition common to chondrichthyans and osteichthyans would have been established as a synapomorphy of jawed vertebrates in some lineages of placoderms (Fig. 12). This modification may be functionally linked with the postorbital connection between the palatoquadrate and neurocranium, which is a synapomorphy of the crown gnathostomes [61]. As the caudal oblique muscle could interfere with the postorbital connection between the palatoquadrate and neurocranium, the position of the caudal oblique muscle may have become anterior within the orbit.

Based on the trochlear nerve innervation, the lamprey caudal oblique is likely to be homologous to the gnathostome superior oblique. However, because the number of oculomotor and abducens nerve-innervated muscles differ between the two taxa, it is difficult to identify one-to-one correspondence of the muscles. Nishi [31] suggested that the lamprey ventral rectus is homologous to the gnathostome lateral rectus, and the lamprey caudal rectus corresponds to the additional EOMs, such as the retractor bulbi in gnathostomes. Nishi also suggested that there are two types of muscle duplication patterns of oculomotor nerve-innervated muscles in gnathostomes based on the branching pattern of the nerve. One is that the lamprey dorsal rectus corresponds to the superior rectus and medial rectus in gnathostomes: these muscles are innervated by the dorsal branch of the oculomotor nerve in sharks and lungfishes. The other is that the lamprey anterior oblique corresponds to the medial rectus and inferior rectus, and the lamprey anterior rectus corresponds to the inferior oblique (all innervated by the ventral branch of the oculomotor nerve) in the other gnathostomes. Based on a neurolabeling analysis, Fritzsche et al. [30] modified these ideas to indicate that the lamprey anterior oblique

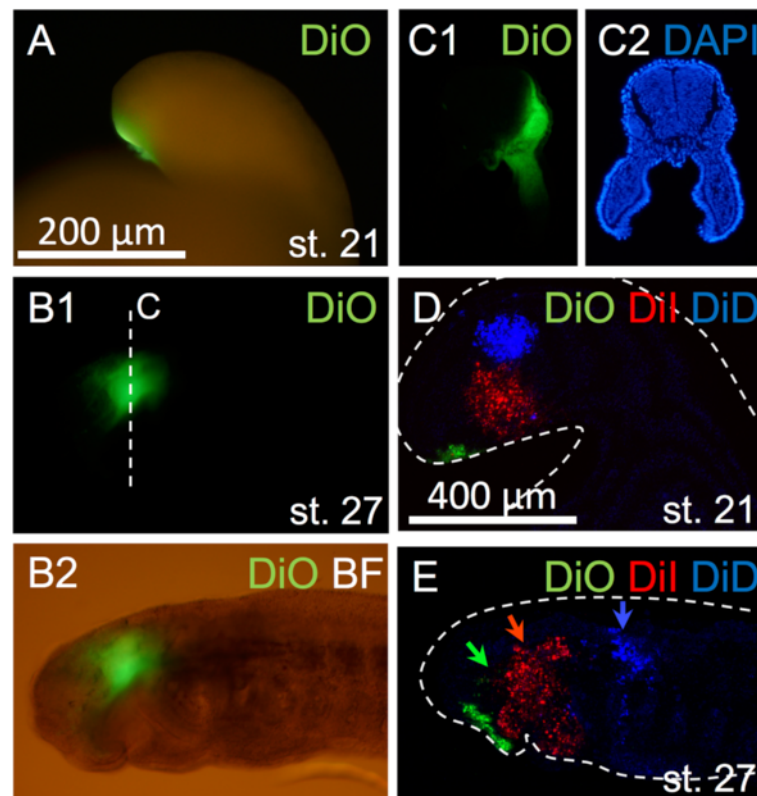


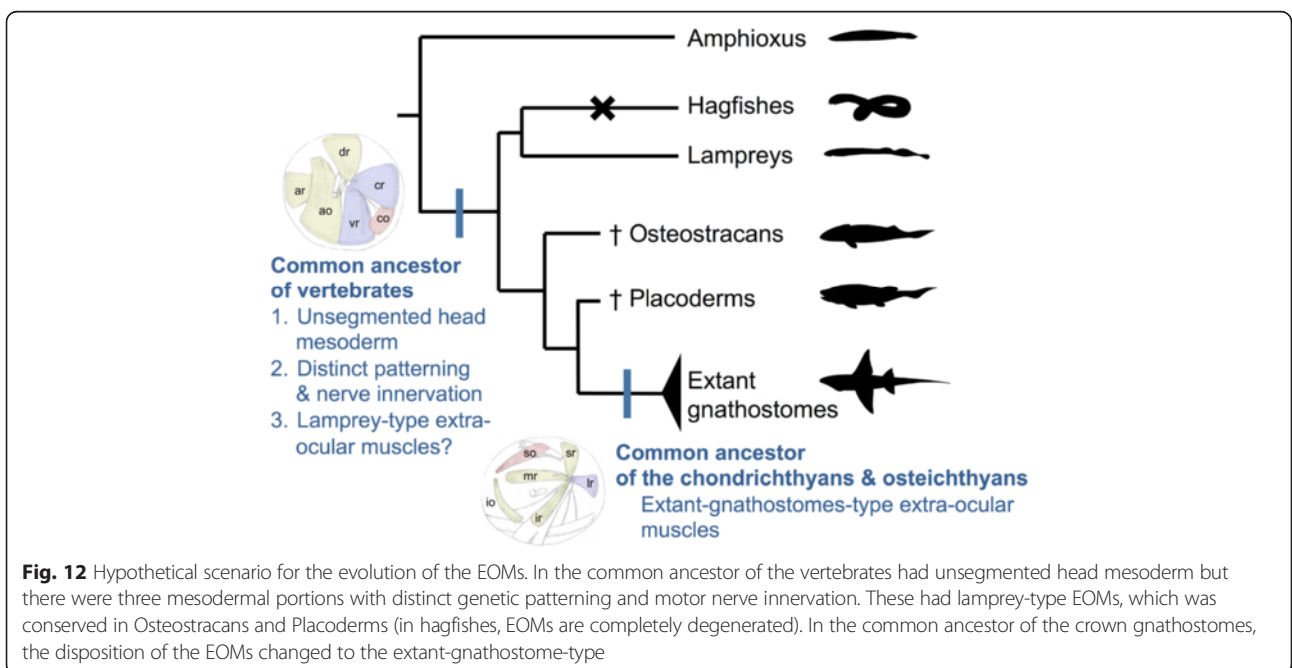
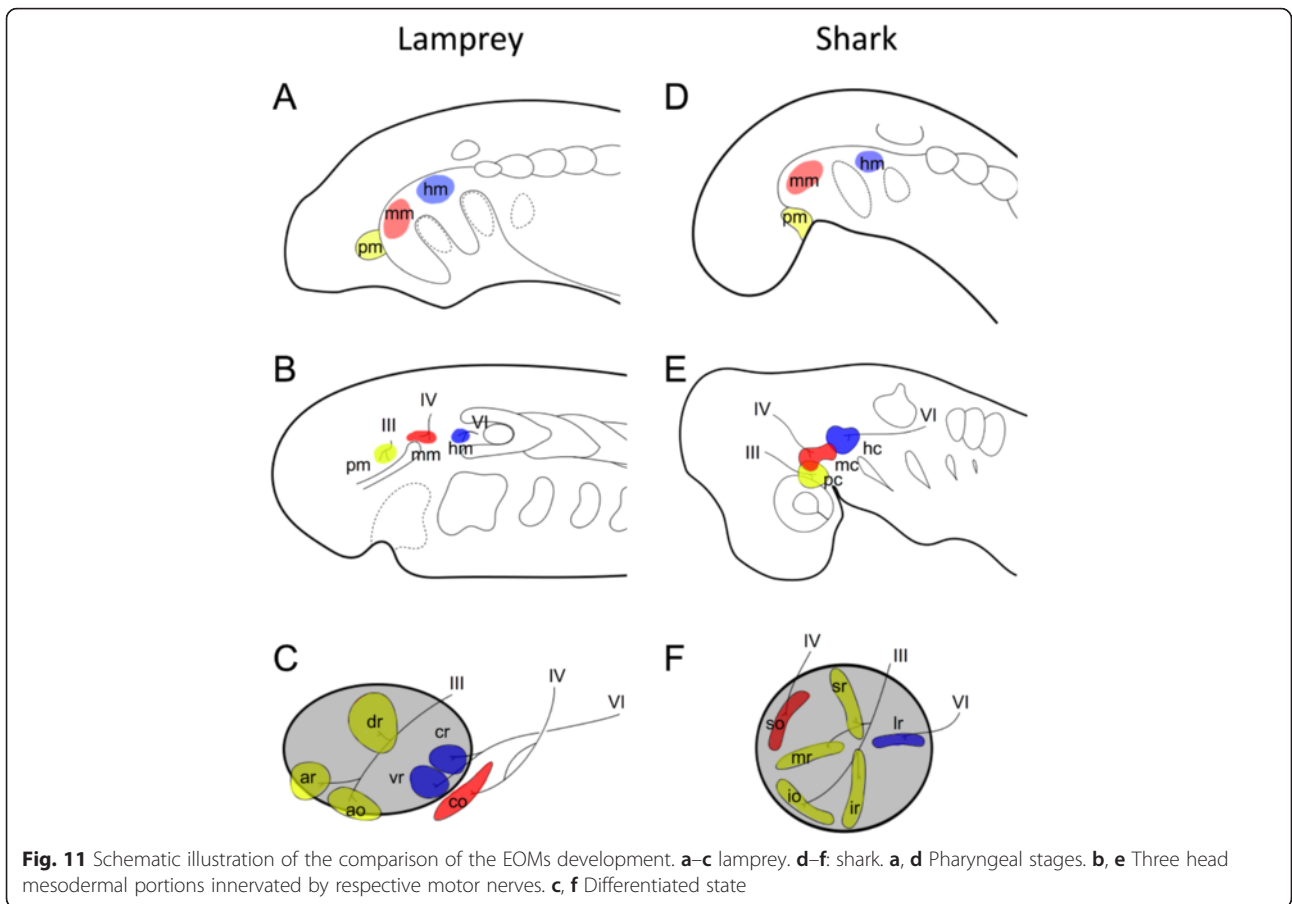
Fig. 10 Dye injections on the head mesoderm. **a** DiO injection into the premandibular mesoderm of the st. 21 embryo. **b** DiO injected sample in st. 27 (**b1**: DiO fluorescence; **b2**: DiO fluorescence and bright field). DiO fluorescence is observed in the periocular region. **c** Section in the dashed line plane in **b1** (**c1**: DiO fluorescence; **c2**: DAPI fluorescence). **d** Three-color dye injections on the three mesodermal portions (premandibular; DiO, mandibular; Dil, hyoid; DiD, respectively). **e** Dye injected sample in st. 27. The three mesodermal portions retained their cohesion

corresponds to the gnathostome inferior oblique, and that the gnathostome medial rectus evolved by duplication of the superior rectus in elasmobranchs and of the inferior rectus in osteichthyans. In the present study, we could not validate the one-to-one correspondence of EOMs, thus we retained the current nomenclature (see also Additional file 1). However, in the lamprey, the dorsal rectus (innervated by the dorsal branch) is differentiated from a cell population distinct from that of the anterior rectus and the anterior oblique (innervated by the ventral branch) (Figs. 5 and 6), providing a clue to determining the correspondence. Also in the chicken [22], there seems to be a close relationship between the medial rectus and inferior rectus, supporting the hypothesis that these two rectus muscles were duplicated in the osteichthyans including amniotes. Further detailed morphological studies on the EOM differentiation in various gnathostomes species are needed to confirm the one-to-one correspondence of EOMs.

Our findings indicate that the latest common ancestors of the vertebrates would have possessed three dorsal head mesodermal portions, although

clear morphological segmentation may not have been present. Although the correspondence between the cranial nerves and the mesodermal components is suggestive of a somitomic type of segmental organization, developmental regionalization and specification do not necessarily indicate the presence of mesodermal segments by themselves. The present data thus support neither presence nor absence of somite-like mesomeres in the ancestral head. Nevertheless, the ancestral dorsal head mesoderm would have also been specified by *Pitx2*, *Gsc* and *Tbx1/10*, and differentiated into EOMs, in a distribution pattern more or less similar to that seen in the modern lampreys.

It remains enigmatic how the head mesoderm and extrinsic eye muscles arose in the vertebrate ancestor. The data from the present study do not resolve this issue. Nevertheless, the present observations suggest that the dorsal head mesoderm is likely to have gone through tripartite regionalization during development by the time of the latest common ancestor of vertebrates. Further comparative developmental studies will be needed to gain insight into the origin of this vertebrate-specific embryonic structure.



Conclusions

We conclude that the EOMs in lamprey developed from three components in the dorsal head mesoderm, which are genetically and regionally specified without segmental boundaries. This developmental mechanism is conserved among vertebrates, indicating that the tripartite origin of EOMs was established in the common ancestor of the vertebrates. Furthermore, our results support the hypothesis that the common ancestor of the vertebrates possessed lamprey-type EOMs, and that the disposition was modified secondarily in the common ancestral lineage of the chondrichthyans and osteichthyans.

Nomenclature

ao anterior oblique
 ar anterior rectus
 cb constrictor buccalis
 co caudal oblique
 cr caudal rectus
 dr dorsal rectus
 elv elevator labialis ventralis
 gV₁ ophthalmicus profundus nerve ganglion
 gV_{2,3} maxillomandibular nerve ganglion
 gVII facial nerve ganglion
 hc hyoid cavity
 hm hyoid mesoderm
 io inferior oblique
 ir inferior rectus
 lr lateral rectus
 mc mandibular cavity
 mm mandibular mesoderm
 mr medial rectus
 oe oral epithelium
 pc premandibular cavity
 pm premandibular mesoderm
 pp phalangeal pouch
 rpe retinal pigment epithelium
 vr ventral rectus
 II optic nerve
 III oculomotor nerve
 IV trochlear nerve
 VI abducens nerve

Additional file

Additional file 1. Homology and developmental patterning of EOMs. (XLS 29 kb)

Competing interests

The authors declare that they have no competing interests.

Authors' contributions

DGS conceived the project, designed and carried out the morphological, immunofluorescence and gene expression studies, and participated in the

drafting of the manuscript. YF carried out the 3D reconstructions. MY participated in the gene expression studies. YY participated in the preparation of larval materials, and helped to draft the manuscript. JK, SK and HW participated in its design and coordination, and helped to draft the manuscript. All authors read and approved the final manuscript.

Acknowledgements

We thank the anonymous reviewers for their valuable comments and suggestions that improved the quality of the article. A preliminary part of this study was carried out under the Medical Research Internship program of Okayama University (MRI). Part of this study was also supported by Japan Society for the Promotion of Science (JSPS); Grant numbers: 13 J00621 (to DGS).

Author details

¹Graduate School of Life and Environmental Sciences, University of Tsukuba, 1-1-1 Tennodai, Tsukuba, Ibaraki 305-8572, Japan. ²Laboratory for Evolutionary Morphology, RIKEN, Kobe 650-0047, Japan. ³Department of Cytology and Histology, Okayama University Graduate School of Medicine, Dentistry and Pharmaceutical Sciences, 2-5-1 Shikata-cho, Okayama 700-8558, Japan. ⁴Sumitomo Besshi Hospital, 3-1 Oji-cho, Niihama, Ehime 792-8543, Japan. ⁵Graduate School of Science and Engineering for Research, University of Toyama, 3190 Gofuku, Toyama 930-8555, Japan. ⁶Center for Medical Science, International University of Health and Welfare, 2600-1 Kitakanemaru, Ohtawara, Tochigi 324-8501, Japan.

Received: 22 February 2016 Accepted: 6 April 2016

Published online: 14 April 2016

References

- Gilland E, Baker R. Conservation of neuroepithelial and mesodermal segments in the embryonic vertebrate head. *Acta Anat.* 1993;148:110–23.
- Holland LZ, Holland ND, Gilland E. Amphioxus and the evolution of head segmentation. *Integr Comp Biol.* 2008;48(5):630–46.
- Kuratani S. Evolutionary developmental biology and vertebrate head segmentation: a perspective from developmental constraint. *Theory Biosci.* 2003;122:230–51.
- Onai T, Irie N, Kuratani S. The evolutionary origin of the vertebrate body plan: the problem of head segmentation. *Annu Rev Genomics Hum Genet.* 2014;15:443–59.
- Neal HV, Rand HW. *Comparative anatomy.* Philadelphia: Blakiston; 1946.
- Brachet A. *Traité d'Embryologie des Verteébrés.* Paris: Masson & Cie, Editeurs; 1935.
- Fraser EA. The head cavities and development of the eye muscles in *Trichosurus vulpecula*, with notes on some other marsupials. *Proc Zool Soc.* 1915;22:299–346.
- Girbert PW. The origin and development of the head cavities in the human embryo. *J Morph.* 1947;90:149–88.
- Girbert PW. The premandibular head cavities in the opossum, *Didelphys virginiana*. *J Morph.* 1954;95:47–75.
- Girbert PW. The origin and development of the human extrinsic ocular muscles. *Cont Embryol.* 1957;36:59–78.
- Jacob M, Jacob HJ, Wachtler F, Christ B. Ontogeny of avian extrinsic ocular muscles. I. A light and electron-microscopic study. *Cell Tissue Res.* 1984;237:549–57.
- Kundrát M, Janaáček J, Martin S. Development of transient head cavities during early organogenesis of the Nile crocodile (*Crocodylus niloticus*). *J Morph.* 2009;270:1069–83.
- Kuratani S, Nobusada Y, Saito H, Shigetani Y. Morphological characteristics of the developing cranial nerves and mesodermal head cavities in sturgeon embryos from early pharyngula to late larval stages. *Zool Sci.* 2000;17:911–33.
- Starck D. Die Metamerie des Kopfes der Wirbeltiere. *Zool Anz.* 1963;170:393–428.
- Wedin B. The origin and development of the extrinsic ocular muscles in the alligator. *J Morph.* 1953;92:303–36.
- Adelmann HB. The development of the premandibular head cavities and the relations of the anterior end of the notochord in the chick and robin. *J Morph Phys.* 1926;42:371–439.

17. Jacobson AG. Somitomeres: Mesodermal segments in the head and trunk. In: Hanken J, Hall BK, editors. *The vertebrate skull*, vol. 1. Chicago: University of Chicago Press; 1993. p. 42–76.
18. Wachtler F, Jacob HJ, Jacob M, Christ B. The extrinsic ocular muscles in birds are derived from the prechordal plate. *Naturwissenschaften*. 1984;71:379–80.
19. Couly GF, Coltey PM, Le Douarin NM. The triple origin of skull in higher vertebrates: a study in quail-chick chimeras. *Dev*. 1993;117:409–29.
20. Noden DM. The embryonic origins of avian cephalic and cervical muscles and associated connective tissues. *Am J Anat*. 1983;168:144–65.
21. Noden DM. Interactions and fates of avian craniofacial mesenchyme. *Dev*. 1988;103(Suppl):121–40.
22. Noden DM, Francis-West P. The differentiation and morphogenesis of craniofacial muscles. *Dev Dyn*. 2006;235:1194–218.
23. Noden DM, Trainor PA. Relations and interactions between cranial mesoderm and neural crest populations. *J Anat*. 2005;207:575–601.
24. Wachtler F, Jacob M. Origin and development of the cranial skeletal muscles. *Bibliothca Anat*. 1986;29:24–46.
25. Koltzoff NK. Entwicklungsgeschichte des Kopfes von *Petromyzon planeri*. *Bull Soc Nat Moscou*. 1901;15:259–89.
26. Neal HV. The history of the eye muscles. *J Morphol*. 1918;30:433–53.
27. Damas H. Recherches sur le développement de *Lampetra fluviatilis* L.—Contribution à l'étude de la céphalogenèse des vertébrés. *Arch Biol Paris*. 1944;55:1–289.
28. Kuratani S, Horigome N, Hirano S. Developmental morphology of the head mesoderm and reevaluation of segmental theories of the vertebrate head: evidence from embryos of an agnathan vertebrate, *Lampetra japonica*. *Dev Biol*. 1999;210:381–400.
29. Sewertzoff AN. Die Kiemenbogennerven der Fische. *Anat Anz*. 1911;38:487–95.
30. Fritzsche B, Sonntag R, Dubuc R, Ohta Y, Grillner S. Organization of the six motor nuclei innervating the ocular muscles in lamprey. *J Comp Neurol*. 1990;294:491–506.
31. Nishi S. Augenmuskulatur. In: Bolk L, Göppert E, Kallius E, Lubosch W, editors. *Handbuch der vergleichenden Anatomie der Wirbeltiere*, Band 5. Wien: Urban und Schwarzenberg; 1938. p. 453–66.
32. Shimazaki S. Kontribuo al la kompara anatomio de okulmuskoloj ĉe ciklostomoj kaj fiŝoj. *Acta Anat Nip*. 1965;40:354–67.
33. Tahara Y. Normal stages of development in the lamprey, *Lampetra reissneri* (Dybowski). *Zool Sci*. 1988;5:109–18.
34. Yamazaki Y, Goto A. Genetic structure and differentiation of four *Lethenteron* taxa from the Far East, detected from allozyme analysis. *Env Biol Fish*. 1998;52:149–61.
35. Yamazaki Y, Yokoyama R, Nishida M, Goto A. Taxonomy and molecular phylogeny of *Lethenteron* lampreys in eastern Eurasia. *J Fish Biol*. 2006; 68:251–69.
36. Adachi N, Kuratani S. Development of head and trunk mesoderm in the dogfish, *Scyliorhinus torazame*: I. Embryology and morphology of the head cavities and related structures. *Evol Dev*. 2012;14:234–56.
37. Ballard WW, Mellinger J, Lechenault HA. A series of normal stages for development of *Scyliorhinus canicula*, the lesser spotted dogfish (Chondrichthyes: Scyliorhinidae). *J Exp Zool*. 1993;267:318–36.
38. Kuratani S, Ueki T, Aizawa S, Hirano S. Peripheral development of cranial nerves in a cyclostome, *Lampetra japonica*: morphological distribution of nerve branches and the vertebrate body plan. *J Comp Neurol*. 1997;384: 483–500.
39. Cerny R, Cattell M, Sauka-Spengler T, Bronner-Fraser M, Yu F, Medeiros DM. Evidence for the prepattern/cooption model of vertebrate jaw evolution. *Proc Natl Acad Sci U S A*. 2010;107:17262–7.
40. Uchida K, Murakami Y, Kuraku S, Hirano S, Kuratani S. Development of the adenyohypophysis in the lamprey: evolution of epigenetic patterning programs in organogenesis. *J Exp Zool B*. 2003;300:32–47.
41. Kusakabe R, Kuraku S, Kuratani S. Expression and interaction of muscle-related genes in the lamprey imply the evolutionary scenario for vertebrate skeletal muscle, in association with the acquisition of the neck and fins. *Dev Biol*. 2011;350:217–27.
42. Tiecke E, Matsuura M, Kokubo N, Kuraku S, Kusakabe R, Kuratani S, Tanaka M. Identification and developmental expression of two *Tbx1/10*-related genes in the agnathan *Lethenteron japonicum*. *Dev Genes Evol*. 2007;217:691–7.
43. Ogasawara M, Shigetani Y, Hirano S, Satoh N, Kuratani S. *Pax1/Pax9*-related genes in an agnathan vertebrate, *Lampetra japonica*: expression pattern of *LjPax9* implies sequential evolutionary events toward the gnathostome body plan. *Dev Biol*. 2000;223:399–410.
44. Kleerekoper H. The sense organ. In: Hardisty MW, Potter IC, editors. *The biology of lampreys*, vol. 2. London: Academic; 1972. p. 373–404.
45. Villar-Cerviño V, Abalo XM, Villar-Cheda B, Meléndez-Ferro M, Pérez-Costas E, Holstein GR, et al. Presence of glutamate, glycine, and γ -aminobutyric acid in the retina of the larval sea lamprey: comparative immunohistochemical study of classical neurotransmitters in larval and postmetamorphic retinas. *J Comp Neurol*. 2006;499:810–27.
46. Suzuki DG, Murakami Y, Escribá H, Wada H. A comparative examination of neural circuit and brain patterning between the lamprey and amphioxus reveals the evolutionary origin of the vertebrate visual center. *J Comp Neurol*. 2015;523:251–61.
47. Suzuki DG, Murakami Y, Yamazaki Y, Wada H. Expression patterns of *Eph* genes in the “dual visual development” of the lamprey and their significance in the evolution of vision in vertebrates. *Evol Dev*. 2015; 17:139–47.
48. Hardisty MW, Rovainen CM. Morphological and functional aspects of the muscular system. In: Hardisty MW, Potter IC, editors. *The biology of lampreys*, vol. 4A. London: Academic; 1982. p. 137–232.
49. Sambasivan R, Gayraud-Morel B, Dumas G, Cimper C, Paisant S, Kelly RG, Tajbakhsh S. Distinct regulatory cascades govern extraocular and pharyngeal arch muscle progenitor cell fate. *Dev Cell*. 1999;16:810–21.
50. Adachi N, Takechi M, Hirai T, Kuratani S. Development of the head and trunk mesoderm in the dogfish, *Scyliorhinus torazame*: II. Comparison of gene expression between the head mesoderm and somites with reference to the origin of the vertebrate head. *Evol Dev*. 2012;14:257–76.
51. De Robertis EM, Fainsod A, Gont LK, Steinbeisser H. The evolution of vertebrate gastrulation. *Dev Suppl*. 1994;117–24.
52. Sander V, Reversade B, De Robertis EM. The opposing homeobox genes *Gooseoid* and *Vent1/2* self-regulate *Xenopus* patterning. *EMBO J*. 2007; 26(12):2955–65.
53. Kelly RG, Jerome-Majewska LA, Papaioannou VE. The del22q11.2 candidate gene *Tbx1* regulates branchiomic myogenesis. *Hum Mol Genet*. 2004;13:2829–40.
54. Schulte-Merker S, Hammerschmidt M, Beuchle D, Cho KW, De Robertis EM, Nüsslein-Volhard C. Expression of zebrafish *gooseoid* and *no tail* gene products in wild-type and mutant *no tail* embryos. *Dev*. 1994;120:843–52.
55. Belo JA, Leyns L, Yamada G, De Robertis EM. The prechordal midline of the chondrocranium is defective in *Gooseoid-1* mouse mutants. *Mech Dev*. 1998;72:15–25.
56. Begemann G, Gibert Y, Meyer A, Ingham PW. Cloning of zebrafish T-box genes *tbx15* and *tbx18* and their expression during embryonic development. *Mech Dev*. 2002;114:137–41.
57. Showell C, Christine KS, Mandel EM, Conlon FL. Developmental expression patterns of *Tbx1*, *Tbx2*, *Tbx5*, and *Tbx20* in *Xenopus tropicalis*. *Dev Dyn*. 2006; 235:1623–30.
58. Garg V, Yamagishi Y, Hu T, Kathirya IS, Yamagishi H, Srivastava D. *Tbx1*, a DiGeorge syndrome candidate gene, is regulated by sonic hedgehog during pharyngeal arch development. *Dev Biol*. 2001;235:62–73.
59. Janvier P. *Les céphalaspides du Spitsberg*. Paris: Centre National de la Recherche Scientifique; 1985.
60. Janvier P. *Early vertebrates*. Oxford: Clarendon; 1996.
61. Young GC. The relationships of placoderm fishes. *Zool J Linn Soc*. 1986; 88:1–57.
62. Young GC. Number and arrangement of extraocular muscles in primitive gnathostomes: evidence from extinct placoderm fishes. *Biol Lett*. 2008;4: 110–4.
63. Brazeau MD. The braincase and jaws of a Devonian ‘acathodian’ and modern gnathostome origins. *Nature*. 2009;457:305–8.
64. Davis SP, Finarelli JA, Coates MJ. Acanthodes and shark-like conditions in the last common ancestor of modern gnathostomes. *Nature*. 2012;486:247–50.
65. Zhu M, Yu XB, Ahlberg PE, Choo B, Lu J, Qiao T, Qu QM, Zhao WJ, Jia LT, Blom H, Zhu YA. A Silurian placoderm with osteichthyan-like marginal jaw bones. *Nature*. 2013;502:188–93.